



Neutron diffraction investigation of the dhcp and hcp iron hydrides and deuterides

V.E. Antonov^a, K. Cornell^b, V.K. Fedotov^a, A.I. Kolesnikov^{a,*}, E.G. Ponyatovsky^a, V.I. Shiryaev^a,
H. Wipf^b

^a*Institute of Solid State Physics, Russian Academy of Sciences, 142432 Chernogolovka, Moscow district, Russia*

^b*Institut für Festkörperphysik, Technische Hochschule Darmstadt, Hochschulstrasse 6, D-64289, Darmstadt, Germany*

Received 18 April 1997; received in revised form 10 June 1997

Abstract

Iron hydride and deuteride with the dhcp metal lattice and iron deuteride with the hcp lattice were prepared under high hydrogen or deuterium pressures and studied by neutron diffraction in a metastable state at ambient pressure and 90 K. The crystal structures of the obtained phases were refined using the Rietveld method. The composition of the dhcp phase is close to FeH_{1.0} or to FeD_{1.0} and its metal lattice contains many stacking faults in agreement with the previous data. Hydrogen or deuterium atoms in this phase occupy all available octahedral interstitial sites in the metal lattice. The composition of the hcp phase is FeD_{0.42±0.04}, deuterium atoms randomly occupying approximately 0.42 octahedral site of the one available per formula unit (L'3 type structure). The hcp phase is identified with the non-magnetic phase observed earlier in the Mössbauer spectra of Fe–H and Fe–D samples at 4.2 K. © 1998 Elsevier Science S.A.

Keywords: Iron hydride; Neutron diffraction

1. Introduction

The iron–hydrogen system has been intensively studied for many decades mainly in order to better understand the strong effect of hydrogen on the mechanical properties of iron and steels. No iron hydrides were observed during these studies and the equilibrium hydrogen solubility in iron at atmospheric pressures was accurately measured and shown to be very low [1]. At the same time, it is interesting to note that there is more and more evidence that iron hydrides belong to the most widely spread substances of the Earth and that they are the main constituents of its core [2–4]. The hydrides, however, are thermodynamically stable only at high pressures exceeding a few GPa and rapidly decompose to α -Fe and molecular hydrogen under ambient conditions. Fortunately, iron hydrides can be retained in a metastable state at atmospheric pressure and low temperatures, if previously cooled at the high pressure below about 150 K, that allows their more detailed examination.

The iron hydride with the composition close to FeH was first synthesized at a hydrogen pressure of 6.7 GPa at

250 °C [5]. The magnetic [6], Mössbauer [7] and X-ray [8] studies on the “quenched” iron hydride samples at ambient pressure showed that it is a ferromagnetic with a double hcp metal lattice. This modification of iron hydride was later observed in the in situ Mössbauer [9] and X-ray [3] measurements at room temperature and hydrogen pressures above about 3.5 GPa.

The T – P phase diagram of the Fe–H system is rather complex [10] and other stable (bcc and fcc) and metastable (hcp) modifications of iron hydrides have also been detected under high pressures and elevated temperatures in the course of the in situ X-ray measurements [11,12]. The Mössbauer investigation revealed [13] that different iron hydrides can also be present at ambient pressure in the “quenched” Fe–H samples prepared at high hydrogen pressures.

This paper presents the results of the neutron diffraction investigation of the “quenched” Fe–H and Fe–D phases with the dhcp and hcp metal lattices.

2. Sample preparation and experimental details

The following is known about the preparation conditions of iron hydrides:

*Corresponding author. Current address: Department of Physics, UMIST, PO Box 88, Manchester M60 1QD, UK.

At around 280 °C and a hydrogen pressure of 5 GPa, there is a ($\alpha + \varepsilon' + \gamma$) triple point in the equilibrium T - P phase diagram of the Fe–H system [10]. The α phase is the low-pressure primary solid solution of hydrogen in bcc α -Fe [10], the ε' phase is the high-pressure low-temperature modification of iron hydride with the dhcp metal lattice¹ and the composition close to FeH [8] and the γ phase is the high-pressure high-temperature form of iron hydride with the fcc metal lattice and unknown composition [10,12]. The temperature of the $\varepsilon' \rightarrow \gamma$ transformation increases with the pressure and reaches about 400 °C at 7 GPa [10].

The $\alpha \rightarrow \varepsilon'$ transition is sluggish and noticeable amounts of non-reacted α -Fe were still observed in the Fe–H samples exposed to the hydrogen pressures beyond 9 GPa at temperatures up to 350 °C [3,8]. The in situ X-ray measurements [12] showed also that the $\alpha \rightarrow \varepsilon'$ transition is a complex process involving formation of an intermediate metastable phase with hcp metal lattice. The hydrogen content of this non-equilibrium hydride called hereafter the ε hydride was not determined.

In the present work, a number of Fe–H and Fe–D samples were prepared by exposing an approximately 50 mg stack of 0.12 mm thick polycrystalline plates of iron to hydrogen or deuterium pressures of 7.1 to 9.2 GPa at temperatures from 100 to 350 °C for 24 h with subsequent cooling to 100 K in the high pressure cell. The method of hydrogenation is described in more detail elsewhere [14]. Each “quenched” sample was X-rayed at 100 K with a DRON-2.0 diffractometer using Fe–K α radiation. Most samples were prepared of carbonyl iron melted under Ar atmosphere, cold rolled, annealed in vacuum at 800 °C for 15 min and quenched in water. A few samples were made of iron purified by zone melting, cold rolled and finally refined in hydrogen gas at 870 °C for 100 h [15].

The X-ray examination showed that all Fe–H and Fe–D samples contained a certain amount of non-reacted α -Fe. The Fe–H samples consisted mainly of the ε' hydride, some of them also contained traces of the intermediate ε phase. All Fe–D samples contained a noticeable amount of the ε phase along with the ε' hydride and α -Fe. The amount of α -Fe in the samples decreased with increasing temperature of hydrogenation. No sound correlation was observed between the amount of the ε phase and the material of the samples or the conditions of their hydrogenation.

One Fe–H sample containing no intermediate ε phase and two Fe–D samples containing the minimum and the maximum amount of this phase were chosen for the neutron diffraction investigation. These samples are referred to as samples No. 1, 2 and 3 hereinafter. The Fe–H sample No. 1 was made of carbonyl iron and loaded with

hydrogen at 7.1 GPa at 325 °C. The Fe–D samples No. 2 and No. 3 were made of carbonyl iron and of higher purity iron, respectively, and both were loaded with deuterium at 9.2 GPa and 350 °C.

The neutron diffraction experiments were performed at 90 K, using the D1B instrument at the ILL, Grenoble, with a PG (002) monochromator and neutrons of a wavelength of $\lambda = 2.5235$ Å. To diminish texture effects, the sample plates were broken under liquid nitrogen into pieces of the order of 0.5 mm across and then heaped in a vanadium holder 2 mm in diameter. We refrained from further comminution of the pieces because the X-ray examination had shown that pounding the Fe–H samples in a mortar results in severe smearing of their diffraction lines presumably due to partial disordering of a stacking of close packed layers in the dhcp ε' hydride, partial transformation of the hcp ε phase to a yet unidentified state and hydrogen redistribution among the phases. For each sample, the neutron diffraction data were collected during 8 h. Every hour the sample holder was rotated through a certain angle, between 25 and 90 °. The background was determined in a separate empty-can measurement and then subtracted from the measured diffraction spectra.

The obtained neutron spectra were analysed using the Rietveld profile refinement technique implemented in the DBWS-9411 computer program [16], which allows the simultaneous refinement of several phases.

3. Results

The experimental data and results of their Rietveld profile analysis are presented in Figs. 1–3 and Tables 1–3. Phase compositions of the samples agreed with those determined by the X-ray examination. Each sample contained a few per cent of non-reacted α -Fe (space group Im3m, $a = 2.683$ Å) contributing to the neutron spectrum with only two peaks, (011) and (002). The α -Fe contributions to the spectra are shown in Figs. 1–3 by solid lines (b) and are not mentioned in the Tables.

The neutron diffraction patterns of the ε' and ε phases contained no new lines in addition to the lines of dhcp and hcp structures, respectively. The crystal structures of these phases therefore belong to the same $P6_3/mmc$ space group as the dhcp and hcp structures of their metal lattices. In the dhcp and hcp structures, there are two types of highly symmetrical interstitial sites conforming the $P6_3/mmc$ space group, the octahedral and tetrahedral ones. Both were analysed for hydrogen or deuterium occupancy when the structures of the ε' and ε phases were refined.

While treating the experimental data for the ε' -FeH_{*x*} and ε' -FeD_{*x*} phases, their hydrogen or deuterium content was set equal to $x = 1$ in accordance with the outgassing measurements of Ref. [13]. Another finding of Ref. [13] was a rather large concentration of faults in the dhcp stacking sequence of close packed iron layers in the ε'

¹This phase was originally mistaken for the hcp one and called the ε hydride [9] in accordance with the notation for iron allotropic modifications.

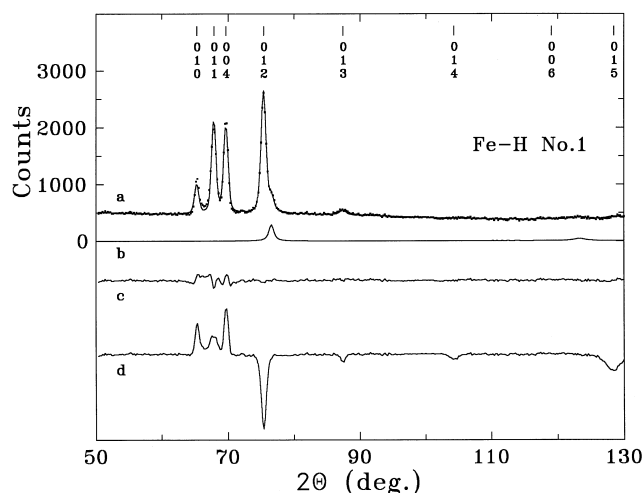


Fig. 1. The neutron diffraction pattern of the Fe-H sample No. 1 measured at 90 K (dots) and the results of its Rietveld refinement involving the ϵ' hydride (the main phase) and α -Fe. The final values of fitting parameters are listed in Table 1. (a) The calculated profile shown as a solid line, (b) the contribution from α -Fe, (c) the difference between the experimental (dots) and calculated (curve a) spectra, (d) the difference between the experimental spectrum and that calculated for hydrogen randomly occupying one half of tetrahedral sites in the dhcp metal lattice of the ϵ' phase, the other fitting parameters being the same as in Table 1. The indices in the upper part of the figure refer to the main ϵ' phase.

phase. To incorporate stacking faults into the calculation scheme with the space group $P6_3/mmc$, a partial occupation of d -sites by iron atoms was allowed along with the occupation of regular a - and c -sites.

The profile analysis showed that the ϵ' phase in the

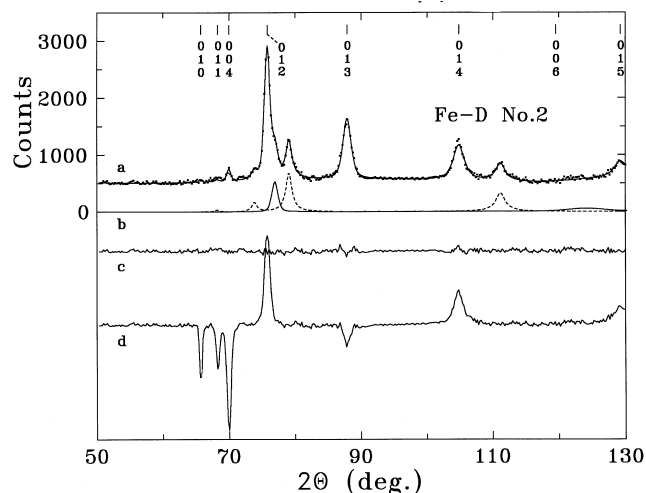


Fig. 2. The neutron diffraction pattern of the Fe-D sample No. 2 measured at 90 K (dots) and the results of its Rietveld refinement involving the ϵ' deuteride (the main phase) and ϵ deuteride and α -Fe. The final values of fitting parameters are listed in Table 2. (a) The calculated profile shown as a solid line, (b) the contributions from the ϵ phase (dashed line) and from α -Fe (solid line), (c) the difference curve, (d) the difference curve in the case of the calculated spectrum assuming tetrahedral deuterium coordination in the ϵ' phase. The indices in the upper part of the figure refer to the main ϵ' phase.

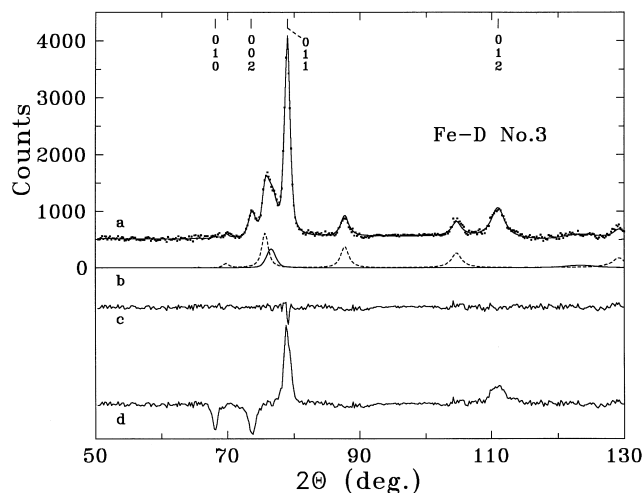


Fig. 3. The neutron diffraction pattern of the Fe-D sample No. 3 measured at 90 K (dots) and the results of its Rietveld refinement involving the ϵ deuteride (the main phase, two blocks with different preferred orientation) and ϵ' deuteride and α -Fe. The final values of fitting parameters are listed in Table 3. (a) The calculated profile shown as a solid line, (b) the contributions from the ϵ' deuteride (dashed line) and from α -Fe (solid line), (c) the difference curve, (d) the difference between the experimental spectrum and that calculated for deuterium randomly occupying 21% tetrahedral interstices in the hcp metal lattice of the ϵ phase, the other fitting parameters being the same as in Table 3. The indices in the upper part of the figure refer to the main ϵ phase.

Fe-H sample No. 1 can be described as a polycrystal with nearly no texture. The refined parameters of this phase are listed in Table 1. Hydrogen occupies only octahedral interstitial sites, both regular ones (f -positions equivalent to the $(1/3, 2/3, 7/8)$ one and called the f_{reg} -positions hereafter) and those due to stacking faults (f_{def} -positions equivalent to the $(1/3, 2/3, 1/8)$ position). The concentration of hydrogen on the “defect” f_{def} -sites is about 6%, that of iron on the “defect” d -sites is about 3% and the ratio of these concentrations is therefore close to 2.

As seen from Table 2, the ϵ' phase in the Fe-D sample No. 2 also can be described as a single homogeneous polycrystal, though with a noticeable texture. The concentration of iron on the “defect” d -sites is higher than in the ϵ' hydride and reaches about 8%. Deuterium occupies only octahedral interstices and its concentration on the “defect” sites is again approximately twice as large as that of iron.

Hydrogen and deuterium have different neutron scattering amplitudes, $b_{\text{H}} = -3.74$ fm and $b_{\text{D}} = +6.67$ fm [17], which leads to different intensity distribution over the diffraction spectra of hydrides and deuterides. Compared to the neutron spectrum of the ϵ' hydride in Fig. 1, the spectrum of the ϵ' deuteride in Fig. 2 exhibits intensive peaks at larger angles. This allowed a more accurate analysis of possible displacements of deuterium atoms from the centres of octahedral interstices, both “regular” and “defect” ones, along the c -axis. The optimization procedure yielded $\delta z = 0.007c$ or 0.06 Å, see Table 2,

Table 1

Positional parameters (x, y, z), isotropic thermal factors (B) and line intensities (I) for the hydride phase in the Fe–H sample No. 1 according to the Rietveld profile refinement analysis of the neutron diffraction data ($\lambda = 2.5235 \text{ \AA}$) collected at 90 K

Phase	Atom	Site	x	y	z	$B (\text{\AA}^2)$	ω	N
ϵ' -FeH _{1.0} (main phase)	Fe	2(<i>a</i>)	0	0	0	0.50	1.000	2.00
P6 ₃ /mmc, $M=4$	Fe	2(<i>c</i>)	1/3	2/3	1/4	0.50	0.935	1.87
$a=2.679 \text{ \AA}$, $c=8.77 \text{ \AA}$	H	4(<i>f</i>)	1/3	2/3	7/8	1.20	0.935	3.74
$c/a=2 \cdot 1.637$	Fe	2(<i>d</i>)	1/3	2/3	3/4	0.50	0.065	0.13
$R_i=4.0\%$	H	4(<i>f</i>)	1/3	2/3	1/8	1.20	0.065	0.26

Pref. orient. 0.98 [001]						
No.	$hk\ell$	HW (deg.)	2θ (deg.)		I_{calc}	I_{obs}
1	010	0.76	65.29		2390	2577
2	011	0.79	67.88		7864	8062
3	004	0.82	69.69		7638	7531
4	012	0.90	75.33		11 659	114 47
5	013	1.11	87.43		585	969
6	014	1.52	104.28		79	17
7	006	2.08	119.12		0	0
8	015	2.59	128.49		546	472

$R_p/R_{\text{ex}}=4.6/5.4$.

The analysis involved two phases, the dhcp ϵ' hydride and α -Fe, the latter being considered as an impurity. N is the number of atoms per formula unit, ω is the site occupation, M is the number of formula units per unit cell, HW is full width at half maximum of the diffraction peak, R_i is Bragg intensity factor, R_p and R_{ex} are the obtained and expected profile factors.

which corresponds to repulsion of the nearest deuterium atoms.

The proposed crystal structure of the ϵ' phase is schematically shown in Fig. 4. The “defect” sites admitted

in the model calculations are alternative positions in the close-packed c -layers of iron atoms and in the close-packed f -layers of hydrogen or deuterium atoms.

The Fe–D sample No. 3 consisted mainly of the hcp ϵ

Table 2

The parameters of the deuteride phases in the Fe–D sample No. 2 according to the Rietveld profile analysis of the neutron diffraction data

Phase	Atom	Site	x	y	z	$B (\text{\AA}^2)$	ω	N
ϵ' -FeD _{1.0} (main phase)	Fe	2(<i>a</i>)	0	0	0	0.40	1.000	2.00
P6 ₃ /mmc, $M=4$	Fe	2(<i>c</i>)	1/3	2/3	1/4	0.40	0.845	1.69
$a=2.668 \text{ \AA}$, $c=8.75 \text{ \AA}$	D	4(<i>f</i>)	1/3	2/3	0.882	0.56	0.845	3.38
$c/a=2 \cdot 1.640$	Fe	2(<i>d</i>)	1/3	2/3	3/4	0.40	0.155	0.31
$R_i=1.6\%$	D	4(<i>f</i>)	1/3	2/3	0.118	0.56	0.155	0.62

Pref. orient. 0.86 [001]						
No.	$hk\ell$	HW (deg.)	2θ (deg.)		I_{calc}	I_{obs}
1	010	0.39	65.69		146	176
2	011	0.60	68.28		10	29
3	004	0.71	69.95		928	981
4	012	1.01	75.80		14543	142 93
5	013	1.46	87.89		10480	104 35
6	014	2.00	104.81		8893	9103
7	006	2.43	119.50		220	231
8	015	2.71	129.24		5466	5429

Phase	Atom	Site	x	y	z	$B (\text{\AA}^2)$	ω	N
ϵ -FeD _{0.42}	Fe	2(<i>c</i>)	1/3	2/3	1/4	0.40	1.00	2.00
P6 ₃ /mmc, $M=2$	D	2(<i>a</i>)	0	0	0	0.60	0.42	0.84
$a=2.583 \text{ \AA}$, $c=4.176 \text{ \AA}$								
$c/a=1.617$	No. <th>$hk\ell$</th> <th>HW (deg.)</th> <th colspan="2">2θ (deg.)</th> <th>I_{calc}</th> <th>I_{obs}</th>	$hk\ell$	HW (deg.)	2θ (deg.)		I_{calc}	I_{obs}	
$R_i=6.0\%$	1	010	0.56	68.16		151	441	
Pref. orient. 1.182 [011]	2	002	0.88	73.87		1094	1126	
	3	011	1.08	79.09		5848	5673	
	4	012	1.70	111.15		4334	4528	

$R_p/R_{\text{ex}}=8.8/6.3$.

The analysis involved three phases, the dhcp ϵ' deuteride and the hcp ϵ deuteride and α -Fe, the latter two being considered as impurities. The measuring conditions and the notation are the same as in Table 1.

Table 3

The parameters of the deuteride phases in the Fe–D sample No. 3 according to the Rietveld profile analysis of the neutron diffraction data

Phase	Atom	Site	<i>x</i>	<i>y</i>	<i>z</i>	<i>B</i> (Å ²)	ω	<i>N</i>
ϵ -FeD _{0.42} (main phase)	Fe	2(<i>c</i>)	1/3	2/3	1/4	0.40	1.00	2.00
P6 ₃ /mmc, <i>M</i> =2	D	2(<i>a</i>)	0	0	0	0.60	0.42	0.84
<i>a</i> = 2.582 Å, <i>c</i> = 4.178 Å								
<i>c/a</i> = 1.618								
<i>R</i> _i = 1.9%								
Pref. orient. 0.54 [011]								
Pref. orient. 0.37 [001]								
No.	<i>hkℓ</i>	HW (deg.)	2 θ (deg.)			<i>I</i> _{calc}	<i>I</i> _{obs}	
1	010	0.87	68.13			157	316	
2	002	0.93	73.52			218	3961	
3	011	1.02	79.01			23785	23583	
4	012	2.43	110.97			8937	9165	
}								
3627								
8937								
9165								
Phase	Atom	Site	<i>x</i>	<i>y</i>	<i>z</i>	<i>B</i> (Å ²)	ω	<i>N</i>
ϵ' -FeD _{1.0}	Fe	2(<i>a</i>)	0	0	0	0.40	1.000	2.00
P6 ₃ /mmc, <i>M</i> =4	Fe	2(<i>c</i>)	1/3	2/3	1/4	0.40	0.845	1.69
<i>a</i> = 2.668 Å, <i>c</i> = 8.75 Å	D	4(<i>f</i>)	1/3	2/3	0.882	0.56	0.845	3.38
<i>c/a</i> = 2·1.640	Fe	2(<i>d</i>)	1/3	2/3	3/4	0.40	0.155	0.31
<i>R</i> _i = 11.9%	D	4(<i>f</i>)	1/3	2/3	0.118	0.56	0.155	0.62
Pref. orient. 0.76 [001]								
No.	<i>hkℓ</i>	HW (deg.)	2 θ (deg.)			<i>I</i> _{calc}	<i>I</i> _{obs}	
1	010	0.90	65.53			47	241	
2	011	0.98	68.12			4	9	
3	004	1.02	69.80			540	756	
4	012	1.18	75.65			5258	5388	
5	013	1.46	87.75			4035	3461	
6	014	1.84	104.69			3673	4132	
7	006	2.17	119.41			125	154	
8	015	2.40	129.16			2498	2818	

 $R_p/R_{ex} = 8.8/5.8$.

The analysis involved four phases, the dhcp ϵ' deuterides with preferred orientation vectors [011] and [001], the hcp ϵ deuteride and α -Fe. The former deuteride was considered as the main phase and the other three phases as impurities. The measuring conditions and the notation are the same as in Table 1.

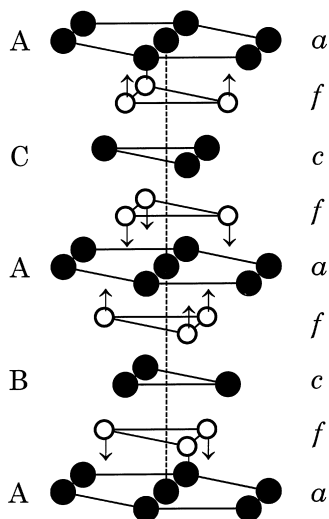


Fig. 4. The crystal structure of ϵ' iron hydride and deuteride. The letters *a*, *c* and *f* mark the layers of equivalent positions in the P6₃/mmc space group originated, respectively, from the positions 2(*a*), 2(*c*) and 4(*f*) with $z \approx 7/8$ listed in Tables 1 and 2. The solid circles show regular positions of Fe atoms, the open circles of H or D atoms. The arrows indicate the directions of displacements of hydrogen (deuterium) atoms from the centres of octahedral interstices. The letters A, B, C represent the standard notation for close-packed layers in the dhcp structure.

phase, as one can see from Fig. 3. The neutron diffraction measurements with the sample holder rotated through different angles showed that this phase was largely present as two blocks of grains with different preferred orientations [011] and [001]. Correspondingly, the Rietveld refinement of the finally obtained spectrum (Fig. 3) involved two blocks of the ϵ phase along with the ϵ' phase and α -Fe. The spectrum of the Fe–D sample No. 3 was actually processed together with that of the Fe–D sample No. 2 because the latter also contained a considerable amount of the ϵ phase. More accurate parameters of the ϵ phase resultant from refinement of the spectrum No. 3 were used to get more accurate parameters of the ϵ' phase while refining the spectrum No. 2 and vice versa in a sort of an iteration procedure.

The refined parameters of the ϵ phase are listed in Table 3. With the given orientation of the sample, the block with preferred orientation [001] contributed mainly to the intensity of the peak (002). This contribution is indicated by a separate line in Table 3 and is seen to be relatively small compared to the integral intensity of the spectrum of another block. Owing to the specific features of neutron scattering by the block [001], the profile fit demonstrated a rather good convergence in spite of the superimposed

diffraction patterns from two blocks with identical crystal structures.

The principal result of the profile fit is that the composition of the ε phase is $\text{FeD}_{0.42}$ and deuterium randomly occupies octahedral interstices in its hcp metal lattice.

To estimate the accuracy with which the deuterium content of the ε - FeD_x phase was determined, calculations were performed with fixed values of x ranging from 0.2 to 0.6. The agreement between the experimental and calculated spectra became visually, qualitatively worse with $x \leq 0.37$ and $x \geq 0.45$. Additionally, a value of $x \approx 0.39$ was obtained for the block [001] from the profile analysis of one of the spectra measured at a certain rotation angle of the sample holder and exhibiting the maximum contribution from this block. It can be concluded therefore that the deuterium content of the hcp ε phase lies within $x = 0.42 \pm 0.04$.

4. Discussion

Every parameter of the crystal structures of the ε' and ε phases described in the previous section results from a stable solution of the Rietveld profile refinement problem. The total number of fitting parameters involved in the calculations is, however, rather large and some of them are interrelated. Further substantiation of the obtained data on a qualitative level or on physical grounds could therefore noticeably add to their reliability.

4.1. The octahedral coordination of hydrogen and deuterium in the ε' and ε phases

Because of the small radius of hydrogen atoms in hydrides of transition metals, hydrogen occupies only interstitial sites in their metal lattices. In the hydrides with close packed metal lattices, these are either octahedral or tetrahedral sites [18]. As is seen from the difference curves (d) in Figs. 1–3, the model with tetrahedral hydrogen (deuterium) coordination is qualitatively inconsistent with experiment for both the ε' and ε phases. The result of the profile fits that all hydrogen (deuterium) in these phases sits on octahedral positions and fills no tetrahedral ones, looks quite reasonable in this respect.

Moreover, the octahedral hydrogen coordination in the ε' and ε phases agrees with the empiric rule [18] to say that hydrogen should occupy octahedral interstices in close packed metal lattices of hydrides of transition metals positioned to the right of the vanadium group in the Periodic Table. The rule has had no exclusions so far and it has clear physical grounds: The atomic radii of transition metals and, correspondingly, the size of interstices decrease from left to right in the Periodic Table and, starting with a certain metal, hydrogen atoms can only fit octahedral sites which are larger than tetrahedral sites.

In the case of 3d transition metals (Ti, V, Cr, Mn, Fe, Co, Ni), the hcp hydrides of chromium and manganese and

the fcc hydride of nickel have already been studied and shown to have octahedral hydrogen coordination (see [19]) in agreement with the rule [18]. With the same hydrogen coordination in the dhcp and hcp iron hydrides established in the present work, there is practically no doubts that the yet unexplored fcc hydride of iron [12] and the hcp and fcc hydrides of cobalt [14] should also have hydrogen on octahedral sites.

4.2. The absence of atomic and magnetic superstructure in the ε' and ε phases

The use of neutrons with a rather large wavelength $\lambda = 2.5235 \text{ \AA}$ allowed a more careful examination of the diffraction spectra of the ε' and ε phases in the range of lines with low indices where the effects of ordering should have revealed themselves most clearly. The absence of new lines in these spectra in addition to the lines of the dhcp and hcp structures therefore can be considered as evidence of the absence of any superstructure, either atomic or magnetic, in the ε' and ε phases.

In the case of the ε' phase this result is in line with the proposed octahedral hydrogen coordination, because the composition of this phase is close to FeH and hydrogen just fills up all available octahedral interstices in its dhcp metal lattice. The ε' phase is a ferromagnetic [6] and consequently has no magnetic superstructure.

The absence of atomic ordering in the ε phase is more informative because there are other hcp hydrides to be compared with.

Along with iron, six other transition metals (Cr, Mo, Mn, Tc, Re and Co) are shown to form hexagonal hydrides, all based on the hcp metal lattice [14]. The composition of the chromium and molybdenum hydrides is close to MeH , the other hydrides have broad homogeneity ranges of composition and can be considered as interstitial solid solutions of hydrogen. The solutions TcH_x and MnD_x were studied by neutron diffraction and were shown to form layered octahedral superstructures of the anti- CdI_2 type at x close to $1/2$ [20]. The ε - $\text{FeD}_{0.42}$ phase is thus the first solid solution with the hcp metal lattice which is proved to remain disordered at $x \sim 1/2$.

The absence of magnetic superstructure in the ε iron deuteride is in agreement with the rigid d-band model [14]. The model predicts that hcp iron, an antiferromagnetic with the Néel temperature of about 100 K [21], becomes either a paramagnetic at temperatures down to 0 K or a very weak itinerant ferromagnetic, if loaded with hydrogen up to $x = 0.42$. In both cases it cannot have any magnetic superstructure.

The results of the ^{57}Fe Mössbauer studies of the “quenched” Fe–H and Fe–D foils at 4.2 K [13] allow a conclusion that the ε phase is paramagnetic. As a matter of fact, the only intensive component which sometimes appeared together with the lines of the ε' phase and α -Fe in the Mössbauer spectra of both the Fe–H and Fe–D foils was a non-magnetic component. Additionally, the hydro-

gen content of the non-magnetic phase was roughly estimated in Ref. [13] by the isomer shift of the non-magnetic component with respect to that of (hypothetical) pure hcp ϵ -Fe [22]. The content proved to be of the order of $x=0.3$ which is close to $x\approx 0.42$ of the ϵ phase. And finally, the width of the non-magnetic line was large compared to that of the ϵ' phase and α -Fe. This is just what one can expect of the disordered ϵ phase because of the distribution of hydrogen or deuterium neighbours around the individual iron atoms [13].

As for the ferromagnetic ϵ' phase with $x\approx 1$, its high Curie temperature of $T_c \gg 80$ K and magnetic moment of approximately 2.2 Bohr magnetons per Fe atom [6] are also in line with the rigid d-band model [14]. Despite the rather large magnetic moment, however, the contribution of the magnetic scattering to the intensities of the Bragg peaks of the ϵ' phase is small due to the large coherent nuclear scattering amplitude of $b_{\text{Fe}}=9.45$ fm [17] and due to the steep decrease in the magnetic form factor of Fe with increasing $\sin \theta/\lambda$ ratio [23].

As is seen from Fig. 5, this magnetic contribution did not exceed the experimental scatter for the peaks at $65^\circ < 2\theta < 76^\circ$ and practically vanished at higher angles. The effect of magnetic scattering could be seen better in the neutron spectrum of ϵ' -FeD than in that of ϵ' -FeH owing to the low intensities of (010), (011) and (004) peaks resulting from the nuclear scattering in the deuteride. The Rietveld profile analysis of the neutron data for the Fe–D sample No. 2 showed that of the two limiting cases, with iron magnetic moments directed along and perpendicular to the c -axis of the ϵ' phase, the former is a little more conceivable. Note in this connection that magnetic mo-

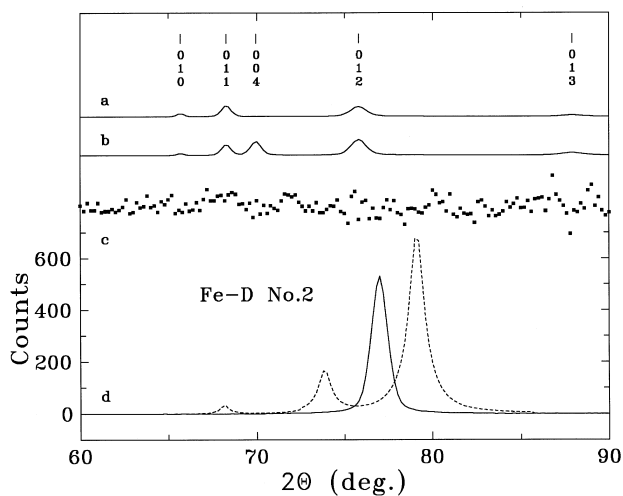


Fig. 5. The calculated contribution from magnetic scattering to the neutron diffraction spectrum of the ϵ' phase in the Fe–D sample No. 2 in the case of iron magnetic moments oriented along the c -axis (curve a) and perpendicular to it (curve b). The difference spectrum (c) and the calculated spectra of impurity phases, α -Fe and the ϵ -deuteride, (d) are given for comparison and represent portions of spectra c and d, respectively, from Fig. 2. The indices in the upper part of the figure refer to the ϵ' phase.

ments are aligned along the c -axis in ferromagnetic hcp cobalt and its hydrides [24].

In view of the remaining uncertainty in the orientation of magnetic moments in the ϵ' -FeD and ϵ' -FeH, we neglected the magnetic contribution to the neutron spectra of these phases while analysing their crystal structure. With any given orientation of magnetic moments, this did not detectably affect the results of the calculations and, in particular, did not change any figure in the final values of the parameters presented in Tables 1 and 2.

4.3. Stacking faults in the ϵ' phase

The dhcp structure belongs to the $P6_3/mmc$ space group and has equal number of “cubic” a -sites and “hexagonal” c -sites positioned correspondingly between two differently stacked close packed layers of the c -sites and between two equally stacked close packed layers of the a -sites, see Fig. 4. The Mössbauer investigation showed [13] that in the ϵ' iron hydrides and deuterides, iron atoms on “hexagonal” sites outnumber those on “cubic” sites by approximately 20% owing to faults in the ideal dhcp stacking sequence.

The presence of stacking faults in the structure of the ϵ' phase is clearly seen in the neutron diffraction spectra as well. As Fig. 6 shows, the intensity of (011) line of the ϵ' hydride and the intensities of (013) and (015) lines of the ϵ' deuteride are much smaller than those calculated for the structures with the ideal dhcp iron lattice. The (011), (013) and (015) diffraction lines are superstructural lines in the case of the hcp lattice which consists of stacked close packed layers of only “hexagonal” c -sites. The decrease in the intensity of these lines therefore can be attributed to formation of an excessive number of “hexagonal” layers

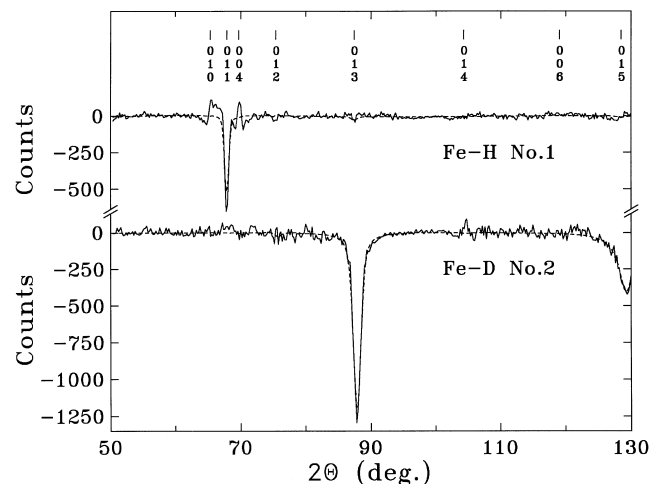


Fig. 6. The difference between the experimental neutron diffraction spectrum (solid line) or between its profile fit (dashed line) and the spectrum calculated under the assumption that the ϵ' phase contained no stacking faults. The latter was obtained by using the same fitting parameters as for the profile fit except that all iron and hydrogen (deuterium) atoms in the ϵ' phase were placed on their regular positions. The indices in the upper part of the figure refer to the ϵ' phase.

in the dhcp iron lattice, which is also in agreement with the Mössbauer data [13]. Since X-ray and neutron diffraction reveal no superstructure in the ε' phase, the excessive “hexagonal” layers should be chaotically distributed over the dhcp lattice, i.e. be stacking faults.

As nothing is known yet about the microscopic structure of the faults in the ε' phase, the neutron diffraction spectra of the ε' hydride and deuteride were calculated using the model which takes the faults into account in no dependence on their microscopic characteristics. Actually, the concentration of iron atoms on d -sites (Tables 1 and 2) represents the mean concentration of any iron layers contributing to diffraction as “defect” ones.

It is seen from Figs. 1, 2 and 6 and from Tables 1 and 2 that the model provides a rather good description of the experimental spectra. Additionally, it yields a value of the hydrogen (deuterium) concentration on “defect” sites approximately twice as large as that of iron for both the ε' hydride and deuteride, which can be considered as a successful self-test. In fact, a replacement of a c -layer of iron atoms by a d -layer, which is just a rotation of the layer through an angle of 60° , will also rotate two adjacent hydrogen (deuterium) layers from f_{reg} -positions to alternative f_{def} -positions. Hydrogen (deuterium) occupies all available octahedral interstices in the structure of the ε' phase. Consequently, the concentration of hydrogen (deuterium) on the “defect” f_{def} -sites must be two times that of iron on the “defect” d -sites if the calculation is self-consistent. As is seen from Tables 1 and 2, this is the case.

The concentration C_d of iron on “defect” d -sites is not directly related to the concentrations of iron on “hexagonal” and “cubic” sites with a ratio of $p \approx 1.2$ determined by Mössbauer spectroscopy [13]. For instance, a dhcp pile of any number of close packed layers containing d -layers instead of c -layers would convert only two “cubic” layers on its boundaries into two “hexagonal” ones. The efficiency of the conversion is maximum with the isolated d -layers, each new atom on d -site resulting in a transfer of two atoms from “cubic” to “hexagonal” positions.

With a given value of $p \approx 1.2$, one can estimate the minimum possible concentration C_d^{min} of iron atoms on d -sites assuming that they form only isolated layers:

$$C_d^{\text{min}} = \frac{p-1}{p+1} \cdot \frac{1}{4} \approx 2.3\%.$$

As is seen from Tables 1 and 2, the profile fit yields $C_d \approx 3\%$ for the ε' hydride and $C_d \approx 8\%$ for the ε' deuteride. Both these values are consistent with $C_d^{\text{min}} = 2.3\%$.

4.4. The deuterium displacements from the ideal octahedral positions in the ε' deuteride

The displacements manifest themselves in a non-monotonous angular dependence of the intensity of diffraction

lines with $\ell \neq 0$ which cannot be compensated by varying the isotropic thermal factor. In the case of the ε' deuteride, however, this effect is largely within the error limits because of the limited quality of the diffraction data and due to the large contribution from stacking faults also to be determined from these diffraction data. The obtained value of $\delta z = 0.007c$ of the deuterium displacements (Table 2) is just a result of a better profile fit.

At the same time, the displacements with positive δz values are very likely to occur on physical grounds.

As is seen from Table 2 and Fig. 4, the positive sign of δz means that the deuterium octahedral layers separated by the “hexagonal” c - or d -layers of iron move apart whereas those separated by the “cubic” a -layers move closer together. The former pairs of deuterium layers are equally stacked and the shortest distance between their atoms is $L_h = c/4 + 2\delta z$, whereas the latter ones are stacked differently and the shortest distance is $L_c = \sqrt{(c/4 - 2\delta z)^2 + a^2/3}$. With $\delta z = 0$, when deuterium atoms sit at the centres of octahedrons, $L_h = 2.188 \text{ \AA}$ which is shorter than $L_c = 2.675 \text{ \AA}$ and $a = 2.668 \text{ \AA}$. The increase in δz thus leads to the increase in L_h which is the shortest distance between any two deuterium atoms in the ε' deuteride. This is the very effect that one can expect in view of the strong long-range repulsive interaction between hydrogen (deuterium) atoms which is one of the main factors governing formation of hydrides and deuterides of transition metals [18].

We therefore suppose that the displacements of deuterium atoms from the centres of octahedral interstices do occur in the ε' deuteride, though the obtained value of $\delta z = 0.007c$ can be considered only as a rough estimation.

5. Summary

Of the four different phases with the dhcp [8], hcp [12], fcc [12] and bcc [11] iron lattices which are known to form in the Fe–H system at high hydrogen pressures, the former two are studied now by neutron diffraction.

The ε' hydride with the dhcp iron lattice is thermodynamically stable at high hydrogen pressures [3,8]. The ε hydride with the hcp iron lattice is formed as an intermediate metastable phase in the course of the transformation of α -Fe to the stable ε' hydride at high pressures and elevated temperatures [12]. Both ε' and ε hydrides are unstable at ambient conditions and rapidly decompose to α -Fe and molecular hydrogen.

In the present work, taking these results as a basis, Fe–H and Fe–D samples consisting mainly of the ε' phase and a Fe–D sample with the predominant ε phase were synthesized of iron and hydrogen or deuterium at pressures of 7.1 to 9.2 GPa and temperatures of 325 to 350 °C, cooled to 100 K under the pressure to prevent hydrogen (deuterium) losses after further lowering the pressure to 1

atm and then studied by neutron diffraction in a metastable state at 90 K. The obtained data were analysed using the Rietveld refinement method.

The investigation showed that hydrogen and deuterium occupy octahedral interstices in the close packed iron lattices of both the ε' and ε phases. The octahedral hydrogen coordination was observed in hydrides of all VI–VIII group transition metals studied so far [19] and is apparently a consequence of a too small size of interstices of another, tetrahedral type [18].

The composition of the ε' phase is close to the stoichiometry FeH or FeD in agreement with the results [13] of chemical analysis. The structure of the ε' phase is characterized by a high concentration of stacking faults. The calculated parameters of the model used to incorporate the faults into the profile refinement of the neutron data are consistent with the ratio of $p \approx 1.2$ of the number of iron atoms in the “hexagonal” and “cubic” close packed layers which was determined by Mössbauer spectroscopy [13]. Hydrogen or deuterium occupies all available octahedral interstices, both regular ones and those due to the stacking faults.

The profile analysis of the neutron spectrum of the ε' deuteride also shows a tendency of the close packed deuterium layers separated by the “hexagonal” iron layers to move apart whereas those separated by the “cubic” iron layers move closer together. The movements lead to an increase in the shortest distance between the neighbouring deuterium atoms which is the very effect to be expected in view of the strong long-range repulsive interaction characteristic of hydrogen (deuterium) atoms in transition metals [18].

According to the profile analysis of the neutron spectrum of the hcp ε -FeD_x phase, its deuterium content is $x = 0.42 \pm 0.04$. Regretfully, this value is not additionally proved by chemical analysis because the sample is inhomogeneous and the content of the other phases cannot be determined accurately enough.

Deuterium randomly occupies octahedral interstices in the hcp iron lattice of the ε -FeD_x. In this respect, the ε phase in the Fe–D system is unlike the earlier studied non-stoichiometric hcp phases TcH_x and MnD_x which form layered superstructures of the anti-CdI₂ type at x values close to 1/2 [20].

The ε -FeD_x exhibits no magnetic superstructure either. The comparison with the results of the Mössbauer studies [13] shows that this phase is paramagnetic at temperatures down to 4.2 K. These findings are in agreement with the rigid d-band model [14] predicting that the incorporation of $x = 0.42$ of hydrogen should transform antiferromagnetic [21] hcp iron to a paramagnetic or to a very weak itinerant ferromagnetic. (The ε' -FeH is a ferromagnetic with a high Curie temperature of $T_c \gg 80$ K and magnetic moment of approximately 2.2 Bohr magnetons per Fe atom [6], which also agrees with the rigid d-band model.)

Acknowledgements

The assistance of Dr. A.W. Hewat and Dr. B. Ouladdiaf, ILL, in conducting the neutron diffraction experiments is greatly acknowledged. The work was supported by the Russian Foundation for Basic Research under a Grant No. 96-02-17522.

References

- [1] J.R.C. da Silva, R.B. McLellan, *J. Less-Common Metals* 50 (1975) 1.
- [2] V.N. Larin, *Hydrided Earth: The New Geology of our Primordially Hydrogen-Rich Planet*, Izd. IMGRE, Moscow, 1975, Polar Publishing, Calgary, Canada, 1993.
- [3] J.V. Badding, R.J. Hemley, H.K. Mao, *Science* 253 (1991) 421.
- [4] T. Yagi, T. Hishinuma, *Geophys. Res. Lett.* 22 (1995) 1933.
- [5] V.E. Antonov, I.T. Belash, V.F. Degtyareva, E.G. Ponyatovskii, V.I. Shiryayev, *Dokl. Akad. Nauk SSSR* 252 (1980) 1384 [Engl. Trans. *Sov. Phys. Dokl.* 24 (1980) 490].
- [6] V.E. Antonov, I.T. Belash, E.G. Ponyatovskii, V.G. Thiessen, V.I. Shiryayev, *Phys. Stat. Sol. (a)* 65 (1981) K43.
- [7] R. Wordel, F.E. Wagner, V.E. Antonov, E.G. Ponyatovskii, A. Permogorov, A. Plachinda, F.E. Makarov, *Z. Phys. Chem. N.F.* 146 (1985) 121.
- [8] V.E. Antonov, I.T. Belash, V.F. Degtyareva, D.N. Mogilyansky, B.K. Ponomarev, V.Sh. Shekhtman, *Int. J. Hydrogen Energy* 14 (1989) 371.
- [9] I. Choe, R. Ingalls, J.M. Brown, Y. Sato-Sorensen, R. Mills, *Phys. Rev. B* 44 (1991) 1.
- [10] V.E. Antonov, I.T. Belash, E.G. Ponyatovskii, *Scripta Metal.* 16 (1982) 203.
- [11] Y. Fukai, A. Fukizawa, K. Watanabe, M. Amano, *Jpn. J. Appl. Phys.* 21 (1982) L318.
- [12] M. Yamakata, T. Yagi, W. Utsumi, Y. Fukai, *Proc. Jpn. Acad.* 68B (1992) 172.
- [13] G. Schneider, M. Baier, R. Wordel, F.E. Wagner, V.E. Antonov, E.G. Ponyatovskii, Yu. Kopilovskii, E. Makarov, *J. Less-Common Metals* 172–174 (1991) 333.
- [14] E.G. Ponyatovskii, V.E. Antonov, I.T. Belash, in: A.M. Prokhorov, A.S. Prokhorov (Eds.), *Problems in Solid-State Physics*, Mir, Moscow, 1984, p. 109.
- [15] D.S. Kamenetskaya, I.B. Piletskaya, V.I. Shiryayev, *High purity iron*, Metallurgizdat, Moscow, 1978 [in Russian].
- [16] R.A. Young, A. Sakthivel, T.S. Moss, C.O. Paiva-Santos, *DBWS 9411 User's Guide*, Georgia Institute of Technology, Atlanta, 1995.
- [17] L. Koester, H. Rauch, E. Seymann, *Atomic Data and Nuclear Data Tables* 49 (1991) 65.
- [18] V.A. Somenkov, S.Sh. Shil'stein, *Z. Phys. Chem. N.F.* 117 (1979) 125.
- [19] V.A. Somenkov, V.P. Glazkov, A.V. Irodova, S.Sh. Shilstein, *J. Less-Common Metals* 129 (1987) 171.
- [20] S.Sh. Shilstein, V.P. Glazkov, A.V. Irodova, V.A. Somenkov, V.E. Antonov, E.G. Ponyatovskii, *Z. Phys. Chem. N.F.* 146 (1985) 129.
- [21] H. Ohno, *J. Phys. Soc. Jpn.* 31 (1971) 92.
- [22] D.L. Williamson, S. Bukshpan, R. Ingalls, *Phys. Rev. B* 6 (1972) 4194.
- [23] C.G. Shull, E.O. Wollan, W.C. Koehler, *Phys. Rev.* 84 (1951) 912.
- [24] I.T. Belash, V. Yu. Malyshev, B.K. Ponomarev, E.G. Ponyatovskii, A. Yu. Sokolov, *Fiz. Tverd. Tela* 28 (1986) 1317 [Engl. Transl. *Sov. Phys. Solid State* 28 (1986) 741].